Journal of Engineering and Applied Sciences 12 (19): 5012-5017, 2017
ISSN: 1816-949X

Determination of Active Pressure Exerted on Retaining Walls with a Circular Failure Wedge Using the Horizontal Slices Method in Cohesive-Frictional Soil

[1]Mojtaba Ahmadabadi, [1]Mohammad Karim Faghirizadeh, [2]Samad Hosseini and [3]Misagh Naghibi
[1]Department of Civil, Faculty of Engineering, Shiraz Art Institute of Higher Education, Shiraz, Iran
[2]University of Shiraz, Shiraz, Iran
[3]Sharif University, Tehran, Iran

Abstract: The current study used the horizontal slices method to develop a new formulation to calculate active pressure on retaining walls. In this method, the failure wedge is assumed to be circular in cohesive-frictional soil. In addition to the formula, graphs are provided to determine the center and radius of failure without need for calculation to determine the pressure exerted on the retaining wall. A comparison of the results of the proposed method with previous methods shows that the active pressure calculated using a circular failure wedge was higher than when using a plate failure wedge; confirming the importance of the circular failure wedge. The proposed method can calculate the shear force between the slices while previous methods often ignored the shear force between slices and cohesion. The proposed method can be used to calculate the pressure distribution along the height of the wall and determine the resultant forces.

Key words: Retaining walls, horizontal slices method, active resultant pressure, critical failure wedge angle, circular wedge failure, cohesive-frictional

INTRODUCTION

The exact calculation of the active pressure of soil significantly decreases the cost of construction of retaining walls. Several methods have been used for this and each make assumptions. These methods include the infinity method, theory of plasticity (Rankine, 1857), theory of elasticity and experimental methods.

The limit equilibrium method is a subset of plasticity theory. The limit equilibrium approach investigates several mechanisms for the failure surface. Kashani (1979) provided an equation to determine the critical wedge failure angle by Mononobe and Matsuo (1929) method. Cheng (2003) investigated active pressure distribution for vertical walls. Ahmadabadi and Ghanbari (2009), Ghanbari and Ahmadabadi (2010a-c) calculated the active pressure of soil. Most methods have considered the failure surface as a plate. Ghanbari and Taheri (2012) examined the effect of overhead in cohesive soil. Vieira (2014) examined the two-line failure wedge and assumed the soil was non-cohesive.

Lin (2015) assumed the failure wedge to be a plate and the backfill soil was assumed to be sloped. The present study calculated the net force exerted by each slice on a wall based on the horizontal slices method by dividing the statistical failure mass into a set of parallel slices and establishing static equilibrium on all slices. The most critical point along the failure circle was also calculated and equations and graphs are provided to determine the center and radius of failure circle. A method that can increase the active pressure in the equilibrium state is of interest to researchers.

MATERIALS AND METHODS

Horizontal slices method with circular failure wedge failure in cohesive frictional soil: In the horizontal slices method, the high surfaces of the failure line can be divided into a number of horizontal slices (Shahgholi *et al*., 2001). The assumptions of the proposed method are as follows:

- Analysis is based on the limit equilibrium method
- The surface of failure crosses over wall feet
- The impact point of force N is from the bottom piece
- Soil mass is considered homogeneous

Figure 1 shows a retaining wall with backfill that has been divided into horizontal parts with a failure wedge in the form of the arc of a circle. The forces exerted on slice

Corresponding Author: Mojtaba Ahmadabadi, Department of Civil, Faculty of Engineering, Shiraz Art Institute of Higher Education, Shiraz, Iran

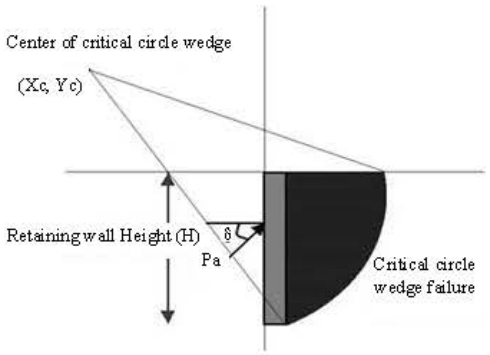

Fig. 1: Retaining wall with a circular failure wedge

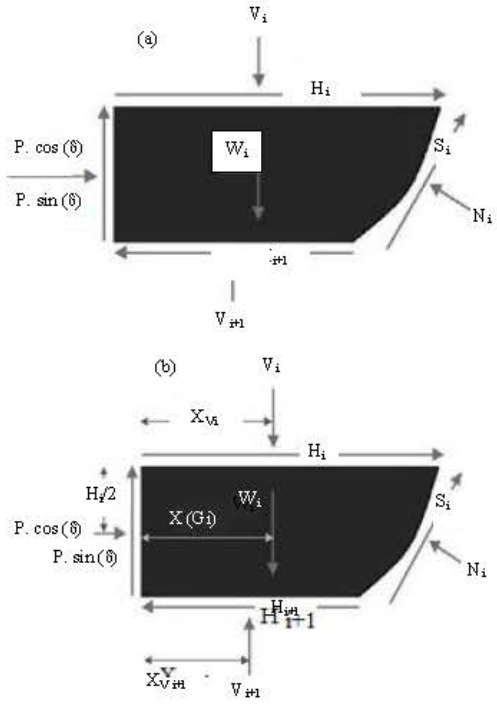

Fig. 2: Forces and impact point on the ith slice

i and the impact point of the forces on the wall are shown in Fig. 2. By considering the large number of slices (1000 horizontal slices), the element can be assumed to be linear. The forces exerted are shown in Fig. 3. If backfill has n horizontal slices of equal height, the height of each slice becomes:

$$h_i = \frac{H}{n} \quad (1)$$

The radius of the circular failure wedge can be calculated as:

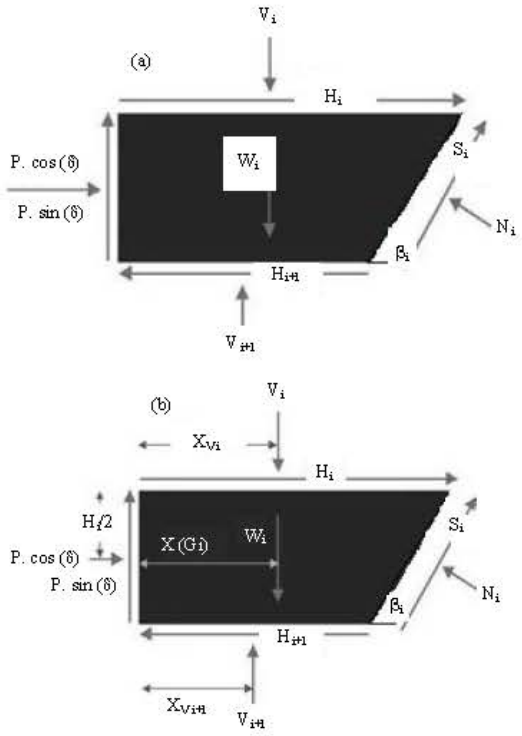

Fig. 3: Forces and impact point on the ith slice of the equivalent horizontal element

$$R = \left|\sqrt{X_c^2 + (H \pm Y_c)^2}\right| \quad (2)$$

In Fig. 3, distances x_i and x_{i+1} can be obtained as:

$$x_i = \left|\sqrt{R^2 + (Y_c - (i-1)\times h_i)^2}\right| \quad (3)$$

$$x_{i+1} = \left|\sqrt{R^2 + (Y_c - (i-1)\times h_i)^2}\right| \quad (4)$$

The impact point of vertical forces below and above each element can be obtained using Eq. 5 and 6 as:

$$X_{vi} = \frac{X_i}{2} \quad (5)$$

$$X_{v\,i+1} = \frac{X_{i+1}}{2} \quad (6)$$

Distance x_{Gi} of the impact point of the element weight where $x_i \leq x_{i+1}$ can be calculated using Eq. 7 otherwise it can be obtained using Eq. 8:

Table 1: Equations and unknowns for horizontal slices method

Unknowns	Number	Equations	Number
H_i: Inter-slice shear force	n	$\sum F_x = 0$ For each slice	n
N_i: Normal forces at base of each slice	n	$\sum F_y = 0$ For each slice	n
S_i: Shear forces at base of each slice	n	$\sum M_o = 0$ For each slice	n
P_i: Net force on wall	n	$Si = N_i(\tan f) + C$ For each slice	n

$$x_{Gi} = \frac{x_i + x_{i+1}}{2} \tag{7}$$

$$x_{Gi} = \frac{\frac{x_{i+1}^2}{2} + \left(\frac{|x_i - x_{i+1}|}{2} \times \left(x_{i+1} + \frac{|x_i - x_{i+1}|}{3}\right)\right)}{x_{i+1} + \frac{|x_i - x_{i+1}|}{2}} \tag{8}$$

The weight of each slice i is w_i and assuming $x_i \leq x_{i+1}$ can obtained using Eq. 9; otherwise it can be obtained using Eq. 10:

$$w_i = \left(\frac{x_i + x_{i+1}}{2}\right) \times h_i \times \gamma \tag{9}$$

$$w_i = \left(xi + \frac{|x_i + x_{i+1}|}{2}\right) \times h_i \times \gamma \tag{10}$$

Additionally, vertical stresses v_i and v_{i+1} below and above each element, respectively can be calculated using Eq. 11 and 12. For inclined walls the equations proposed by Segrestin (1992) or Ahmadabadi *et al*. (2016) should be used in place of Eq. 11 and 12:

$$v_i = \gamma \times (i-1) h_i \tag{11}$$

$$v_{i+1} = \gamma \times (i) h_i \tag{12}$$

To calculate the pressure exerted on retaining walls as shown in Fig. 3, there are four unknowns (Ni, Hi, Si, Pi) for each slice. The same number of equations should be formulated so that the unknowns can be obtained as two equilibrium equations in the horizontal vertical direction, an equilibrium equation for the anchors and an equation of the relationship between the vertical and shear yield stress in the horizontal surfaces between slices. Table 1 shows the 4n unknowns and 4n equations. The first three equations of Table 1 are as follows:

$$H_i - H_{i+1} + S \times \cos\beta - N \times \sin\beta + P \times (\cos\delta \times \cos\theta + \sin\delta \times \sin\theta) = 0 \tag{13}$$

$$-v_i + v_{i+1} - w_i + S \times \sin\beta + N \times \cos\beta + P \times (\sin\delta \times \cos\theta - \sin\delta \times \sin\theta) = 0 \tag{14}$$

$$N \times \left(\sin\beta \times \left(H - \left(i \times \left(\frac{H}{n}\right)\right)\right) + \cos\beta \times \left(x_2 + \left(\frac{x_3}{2}\right)\right)\right) - H_i \times \left(H - \left((i-1) \times H\right)\right) + H_{i+1} \times \left(H - (i \times H)\right) + S \times \left(\sin\beta \times \left(X_2 + \left(\frac{X_3}{2}\right)\right) - \cos\beta \times \left(H - i\left(\frac{H}{n}\right)\right)\right) - P \times \cos\delta \times \left(\cos\theta \times \left(H - i \times \left(\frac{H}{n}\right)\right) - \sin\theta \times D_h\right) - v_i \times x_{vi} + v_{i+1} \times x_{vi+1} - W_i \times XG_i = 0 \tag{15}$$

$$S_i = N_i\left(\tan\phi + cl_i\right) \tag{16}$$

where, W_i is weight of the ith slice. The fourth equation in Table 1 is the yield criterion of the Mohr-Coulomb used for points on the failure wedge. These equations obtain the pressure exerted on the wall and the horizontal force between slices (H_i). The total force exerted on wall P is the sum of P_i obtained from each element as.

RESULTS AND DISCUSSION

Results of proposed method in frictional cohesive soils: Analysis carried out on frictional cohesive soil is divided into three main groups. The aim of the analysis is to present executable graphs that do not require lengthy calculation. The analysis is based on the specifications listed in Table 2. The first group investigated the circular failure wedge radius in frictional cohesive soil and found that as the cohesion and internal friction angle of soil increased, the failure circle radius increased (Fig. 4).

The second group examined the center of the circle of the failure wedge. Figure 5 shows that as the cohesion and internal friction angle of soil increased, the distance to the center of the circle of failure increased.

The third series of analyses examined the pressure exerted on the wall. Figure 6-8 show changes in the pressure exerted versus the internal friction angle. In each graph, these investigations were done for five modes of cohesion. Figure 6 shows the graph for $\delta = \phi/6$, Fig. 7 for $\delta = \phi/3$ and Fig. 8 for $\delta = 2\phi/3$. As seen in all graphs, increasing the cohesion, internal friction angle and angle of friction between soil and wall decreased the pressure on the wall.

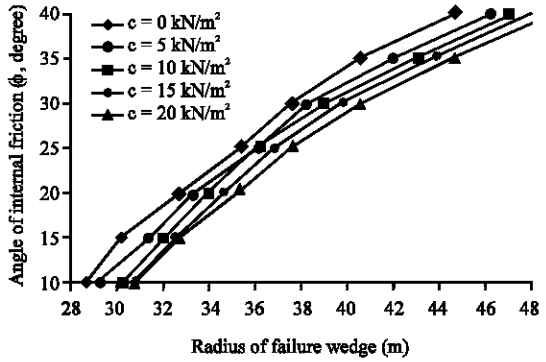

Fig. 4: Change in radius of circular failure wedge versus the internal friction angle of soil at $\delta = 2\phi/3$; H = 10 m, $\gamma = 20$ kN/m^3, $\delta = 2/3\ \phi$

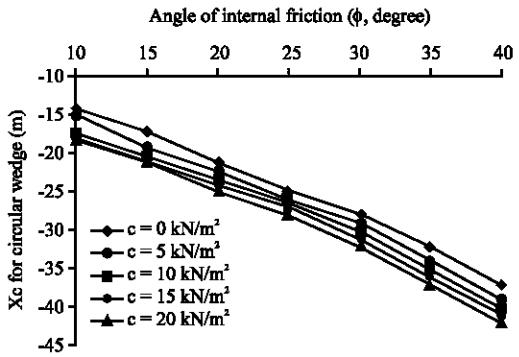

Fig. 5: Change in radius of circular failure wedge versus internal friction angle of soil at $\delta = 2\phi/3$; H = 10 m, $\gamma = 20$ kN/m^3, $\delta = 2/3\ \phi$

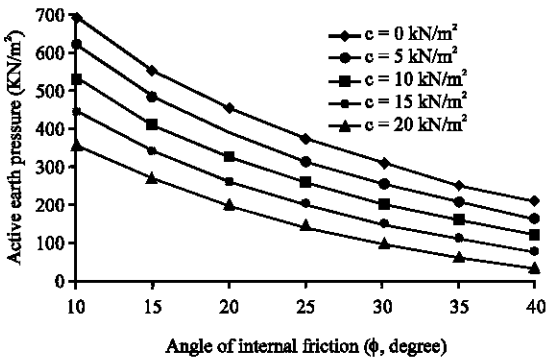

Fig. 6: Change in pressure exerted on retaining wall versus internal friction angle of soil at $\delta = \phi/6$; H = 10 m, $\gamma = 20$ kN/m^3, $\delta = \phi/6$

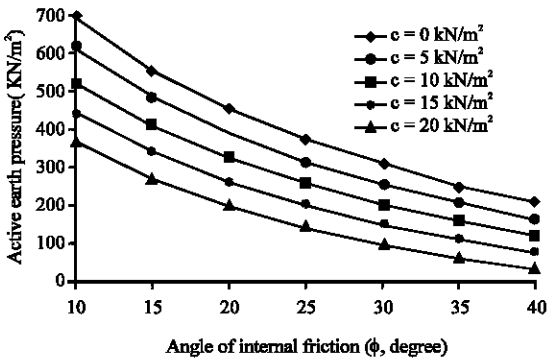

Fig. 7: Change in active pressure exerted on retaining wall versus internal friction angle of soil at $\delta = \phi/3$; H = 10 m, $\gamma = 20$ kN/M^3, $\delta = \phi/3$

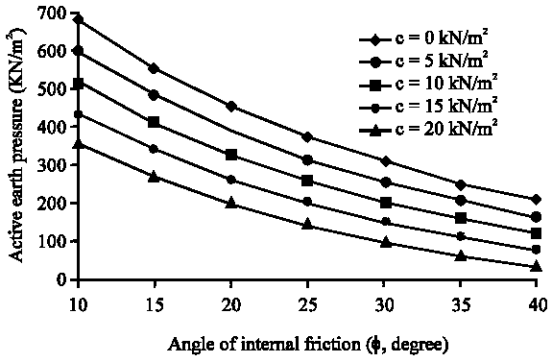

Fig. 8: Change in active pressure exerted on retaining wall versus internal friction angle of soil at $\delta = 2\phi/3$; H = 10 m, $\gamma = 20$ kN/M^3, $\delta = \phi/3$

Table 2: Characteristics of wall and soil used for circular failure wedge

Variables	Values
Height of wall (m)	10 m
Friction angle between wall and backfill soil(δ°)	1/6 ϕ, 1/3 ϕ, 2/3 ϕ
Soil density (γ)	20 kN/m^3
Soil cohesion (C)	0-20 kN/m^2
Internal angle of soil friction (φ°)	10°-40°

Comparison of results of proposed method with results of other researchers: Several methods have been proposed to examine the pressure exerted on the retaining wall. Each method has certain conditions and restrictions which must be adhered to when calculating the pressure on the wall. The results presented use limit equilibrium and the assumptions of the horizontal slices method for a wall in cohesive soil. The results of the proposed method were then compared with the results of previous research under equal conditions.

The methods by Rankine (1857), Das and Puri (1996), Cheng (2003), Ghanbari and Ahmadabadi (2010a-c) were used to verify the equations. The results are shown in Table 3-5. In the proposed approach, the failure wedge is an arc of a circle for which center and radius are specified; there in the circular failure wedge, there is no concept of failure wedge angle. Under all circumstances, the pressure exerted on the wall and the circular failure wedge were more critical to the calculations than the other methods.

Table 3: Comparison of results of proposed method with those by Ghanbari and Ahmadabadi (2010), versus change in friction angle between soil and wall (H = 10 m, C = 0 kN/m^2, γ = 20 kN/m^3)

ϕ	Proposed method	Ghanbari and Ahmadabadi (2010)	Coulomb
δ = 0			
20	499/40	490/3	490/3
25	412/93	405/9	405/8
30	338/84	333/66	333/3
δ = 10			
20	462/38	446/7	446/7
25	383/82	372/6	372/6
30	316/67	309/08	308/45
δ = 20			
20	455/02	426/9	426/9
25	374/96	357/4	357/4
30	309/41	297/9	297/31

Table 4: Comparison of results of proposed method with those by Ghanbari and Ahmadabadi (2010), Rankine (1857) versus change in cohesion (H = 10 m, δ = 0°, γ = 20 kN/m^3)

ϕ	Proposed method	Ghanbari and Ahmadabadi (2010)	Rankine (1857)
C = 0 kN/m^2			
20	499/40	490/3	490
25	412/93	405/9	406/0
30	338/84	333/66	333
C = 10 kN/m^2			
20	357/11	350/2	350/1
25	283/87	278/4	279/0
30	222/22	218/19	217/76
C = 20 kN/m^2			
20	214/82	210/2	210/4
25	154/88	151/0	151/5
30	105/61	102/72	102/34

Table 5: Comparison of results of proposed method with those by Ghanbari and Ahmadabadi(2010), Cheng (2003) and Das and Puri (1996) versus change in cohesion (H = 10 m, δ = 10°, γ = 20 kN/m^3

ϕ	Proposed method	Ghanbari and Ahmadabadi (2010)	Cheng (2003)	Das and Puri (1996)
C = 0 kN/m^2				
20	462/38	446/7	440/0	446/74
25	383/82	372/6	366/9	372/61
30	316/67	309/08	303/7	308/46
C = 10 kN/m^2				
20	332/98	318/1	313/2	314/36
25	265/94	255/0	251/1	243/79
30	209/39	201/84	198/1	184/62

CONCLUSION

The following conclusions can be drawn from the comparisons presented in this study. For retaining walls, new formulation with a circular wedge was presented with 4n equations and 4n unknowns. The pressure exerted on the walls, the center of the circular wedge, the radius of the circular wedge and the shear force between the slices for cohesive frictional soil could be obtained using this method. The proposed method has the advantage of considering the soil as frictional and cohesive. It can also calculate the pressure distribution along the wall height. The proposed method can be upgraded to for seismic mode and soil reinforcement.

The graphs formulated in this study were developed using the proposed method. The pressure exerted on wall was calculated without having to develop a formula. These graphs shows that as the cohesion, internal friction angle of the soil and angle of friction between the soil and wall increase, the pressure on the wall decreases. The equations were verified by comparison with the methods by Rankine (1857), Das and Puri (1996), Cheng (2003), Ghanbari and Ahmadabadi (2010a-c). The results showed good convergence with the previous results. The active pressure in circular wedge mode was about 5% higher than for a plate wedge and indicates that the circular wedge was more critical to the calculation than the plate wedge. The results show that by decreasing the internal friction angle and cohesion increased the difference between the circular failure wedge and plate failure wedge.

REFERENCES

Ahmadabadi, M. and A. Ghanbari, 2009. New procedure for active earth pressure calculation in retaining walls with reinforced cohesive frictional backfill. Geotext. Geomembr., 27: 456-463.

Ahmadabadi, M., G. Namvarchi, M. Sharifi and M. Rezaei, 2016. Assessment of shear strength and vertical stress variations in cohesive-frictional soil slopes. J. Eng. Appl. Sci., 11: 292-296.

Cheng, Y.M., 2003. Seismic lateral earth pressure coefficients for C-f soils by slip line method. Comput. Geotech., 30: 661-670.

Das, B.M. and V.K. Puri, 1996. Static and dynamic active earth pressure. Geotech. Geol. Eng., 14: 353-366.

Ghanbari, A. and M. Ahmadabadi, 2010a. New analytical procedure for seismic analysis of reinforced retaining wall with cohesive-frictional backfill. Geosynthetics Intl., 17: 1-16.

Ghanbari, A. and M. Ahmadabadi, 2010b. Active earth pressure on inclined retaining walls in static and seismic conditions. Int. J. Civil Eng., 8: 159-173.

Ghanbari, A. and M. Ahmadabadi, 2010c. Pseudo dynamic active earth pressure analysis of inclined retaining walls using horizontal slices method. Sci. Iran., 17: 1026-3098.

Ghanbari, A. and M. Taheri, 2012. An analytical method for calculating active earth pressure in reinforced retaining walls subject to a line surcharge. Geotext. Geomembr., 34: 1-10.

Kashani, K.Z., 1979. Sliding of gravity retaining wall during earthquakes onsidering vertical accelerations and changing inclination of failure surface. Ph.D Thesis, Massachusetts Institute of Technology, Cambridge, Massachusetts.

Lin, M., 2015. Stability analysis of cutting high loess slope. Proceedings of the International Conference on Mechatronics, Electronic, Industrial and Control Engineering (MEIC 2015), April 1-3, 2015, Atlantis Press, Amsterdam, Netherlands, pp: 380-384.

Mononobe, N. and H. Matsuo, 1929. On the determination of earth pressure during earthquakes. Proc. World Eng. Congr., 9: 179-187.

Rankine, W.J.M., 1857. On the mathematical theory of the stability of earth work and masonry. Proc. R. Soc., 8: 69-87.

Segrestin, P., 1992. Design of sloped reinforced fill structure. Proceedings of the Conference on Retaining Structures, July 20-23, 1992, Institute of Civil Engineering, London, England, pp: 574-584.

Shahgholi, M, A. Fakher and C.J.F.P. Jones, 2001. Horizontal slice method of analysis. Geotech., 51: 881-885.

Vieira, C.S., 2014. A simplified approach to estimate the resultant force for the equilibrium of unstable slopes. Intl. J. Civ. Eng., 12: 65-71.